

Semileptonic D-decays at BESIII

FEN-FEN AN

*Institute of High Energy Physics, Main Building B406
Chinese Academy of Science, Beijing, China*

We present here three analyses of semileptonic D -meson decays based on the 2.92 fb^{-1} of data collected by the BESIII experiment in 2010 and 2011 at the $\psi(3770)$ peak. For the decay $D^+ \rightarrow K^- \pi^+ e^+ \nu_e$, its branching fraction is measured over the whole $m_{K\pi}$ region and in the $\bar{K}^*(892)^0$ window, respectively. A partial wave analysis (PWA) is performed, indicating an S -wave contribution of about 6%. The S -wave phase and the form factors are measured by the PWA and in a model-independent way. For the decay $D^+ \rightarrow \omega e^+ \nu_e$, an improved measurement of the branching fraction is performed and the form factors are determined for the first time. $D^+ \rightarrow \phi e^+ \nu_e$ is searched and an improved upper limit at 90% confidence level is set. For the decay $D^+ \rightarrow K_L e^+ \nu_e$, its branching fraction is measured for the first time and the CP asymmetry is presented. The product of the hadronic form factor and the CKM matrix element, $f_+^K(0)|V_{cs}|$, is also determined in this decay.

PRESENTED AT

The 7th International Workshop on Charm Physics
(CHARM 2015)
Detroit, MI, 18-22 May, 2015

1 Introduction

The analyses presented in this paper are based on the 2.92 fb^{-1} of data sample [1] collected in e^+e^- annihilations at the $\psi(3770)$ peak, which is accumulated with the BESIII detector [2] operated at the double-ring BEPCII collider. At the $\psi(3770)$ peak, D mesons are produced in pairs, thus allowing us to use the technique of tagging D -meson decays [3]. If a decay of one D meson (“tagged decay”) has been fully reconstructed in an event, the existence of another \bar{D} decay (“signal decay”) in the same event is guaranteed. In these analyses D^- is firstly reconstructed in one of the six decay channels: $D^- \rightarrow K^+\pi^-\pi^-$, $D^- \rightarrow K^+\pi^-\pi^-\pi^0$, $D^- \rightarrow K_S^0\pi^-$, $D^- \rightarrow K_S^0\pi^-\pi^0$, $D^- \rightarrow K_S^0\pi^-\pi^-\pi^+$, and $D^- \rightarrow K^+K^-\pi^-$, then semileptonic signals are searched at the recoiling side. Charge conjugated decays are implied similarly.

2 Study of $D^+ \rightarrow K^-\pi^+e^+\nu_e$

The invariant matrix element of the D_{e4} decay of $D^+ \rightarrow K^-\pi^+e^+\nu_e$ is the product of a leptonic and a hadronic current. Thus it’s convenient for us to study the $K\pi$ system in the absence of interactions with other hadrons and the hadronic transition form factors. In this analysis we measure the different $K\pi$ resonant and non-resonant amplitudes that contribute to this decay, which can provide helpful information for the B -meson semileptonic decays. Also we measure the q^2 dependent transition form factors, where q^2 is the invariant mass square of the lepton pair of the $e\nu_e$ system. This can be compared with hadronic model expectations and lattice QCD computations [4].

The signal yield is obtained by simply counting since the background level is lower than 1%. Using the tagging technique introduced in Sec. 1, the branching fractions are measured to be $(3.71 \pm 0.03 \pm 0.08)\%$ over the full $m_{K\pi}$ range and $(3.33 \pm 0.03 \pm 0.07)\%$ in the $\bar{K}^*(892)^0$ region, respectively.

The 4-body D_{e4} decay can be uniquely described by five kinematic variables [5]: $K\pi$ mass square (m^2), $e\nu_e$ mass square (q^2), the angle between the π and the D direction in the $K\pi$ rest frame (θ_K), the angle between the ν_e and the D direction in the $e\nu_e$ rest frame (θ_e), and the angle between the two decay planes (χ). Its PDF can be expressed based on the five variables and then the PWA is performed using an unbinned maximum likelihood method.

The PWA shows that besides the dominant $\bar{K}^*(892)^0$, an S -wave contribution making of the non-resonant background term and the $\bar{K}_0^*(1430)^0$ accounts for $(6.05 \pm 0.22 \pm 0.18)\%$. Other components can be neglected. The $\bar{K}^*(892)^0$ parameters are determined: $m_{\bar{K}^*(892)^0} = (894.60 \pm 0.25 \pm 0.08) \text{ MeV}/c^2$, $\Gamma_{\bar{K}^*(892)^0} = (46.42 \pm 0.56 \pm 0.15) \text{ MeV}/c^2$, and the Blatt-Weisskopf parameter $r_{BW} = 3.07 \pm 0.26 \pm 0.11 \text{ (GeV}/c)^{-1}$. The parameters defining the hadronic form factors are also measured: $r_V = \frac{V(0)}{A_1(0)} = 1.411 \pm 0.058 \pm 0.007$, $r_2 = \frac{A_2(0)}{A_1(0)} = 0.788 \pm 0.042 \pm 0.008$,

$m_V = (1.81_{-0.17}^{+0.25} \pm 0.02) \text{ MeV}/c^2$, $m_A = (2.61_{-0.17}^{+0.22} \pm 0.03) \text{ MeV}/c^2$, $A_1(0) = 0.585 \pm 0.011 \pm 0.017$. m_V is firstly measured for this decay. Corresponding projections over the five kinematic variables are illustrated in Figure 1.

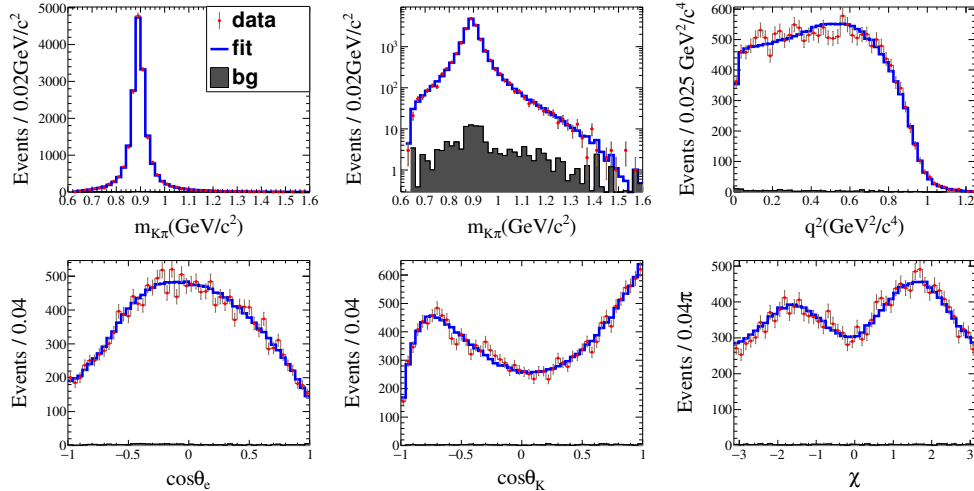


Figure 1: Projections onto each of the kinematic variables, comparing data (dots with error bars) and signal MC weighted by PWA solution (line), assuming that the signal is composed of the S -wave and $\bar{K}^*(892)^0$. The shadowed histogram is the estimated background.

In the above PWA process δ_S depends on $m_{K\pi}$ according to the LASS parameterization. Then we measure δ_S in a model-independent way. We divide the $m_{K\pi}$ spectrum into twelve bins and perform the PWA fit with δ_S in each bin as twelve additional fit parameters (within each bin the phase is assumed to be constant). Figure 2 illustrates the comparison of the model-independent measurement with that based on the LASS parameterization.

In the PWA, the helicity basis form factors are assumed to depend on q^2 according to the spectroscopic pole dominance (SPD) model. In order to achieve a better understanding of the semileptonic decay dynamics, we also measure the form factors in a model-independent way using the projective weighting technique, which is introduced in Ref. [6].

Only candidates in the $\bar{K}^*(892)^0$ region ($[0.8, 1] \text{ GeV}/c^2$) are used, so that we can neglect other components than the $\bar{K}^*(892)^0$ and the non-resonant S -wave. The decay intensity of $D^+ \rightarrow K^- \pi^+ e^+ \nu_e$ can be parameterized by form factors describing the decay into the vector meson $\bar{K}^*(892)^0$: $H_+(q^2, m)$, $H_-(q^2, m)$, $H_0(q^2, m)$, and by an additional form factor $h_0(q^2, m)$ describing the non-resonant S -wave contribution. The form factors are measured by weighting the q^2 distributions based on the angular.

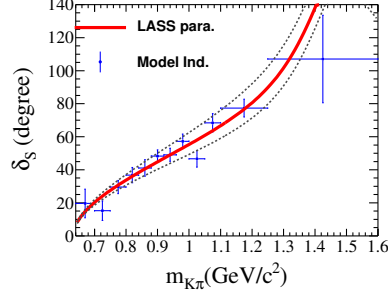


Figure 2: The S -wave phase variation versus $m_{K\pi}$ assuming that the signal is composed of the S -wave and $\bar{K}^*(892)^0$. Model-independent measurement (points with error bars) is compared with the result based on the LASS parameterization (solid line, 1σ deviation is marked by dashed line).

The results are shown in Figure 3. They are consistent with the SPD model with the parameters obtained from the PWA, and with the results reported by CLEO-c [7].

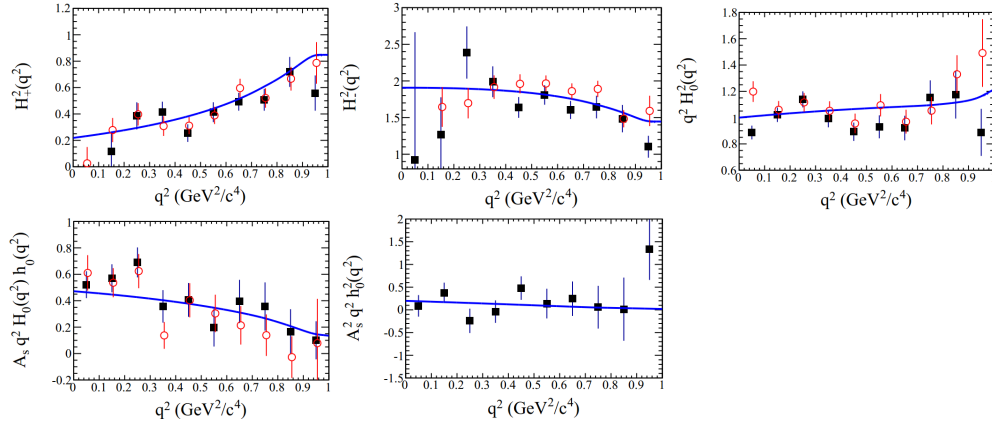


Figure 3: Form factors measured in this work (squares) compared with the CLEO-c results (circles) and with the PWA solution (curves). Error bars represent both statistical and systematic uncertainties.

3 Measurement of the form factors in the decay $D^+ \rightarrow \omega e^+ \nu_e$ and search for the decay $D^+ \rightarrow \phi e^+ \nu_e$

The decay $D^+ \rightarrow \omega e^+ \nu_e$ has similar dynamics as $D^+ \rightarrow \bar{K}^*(892)^0 e^+ \nu_e$. Neglecting the mass of the electron, the transition matrix element of D to vector meson can be decomposed into contributions from one vector $V(q^2)$ and two axial-vector (A_1 ,

$A_2(q^2)$ form factors, where q^2 is the invariant mass square of the $e^+\nu_e$ system. A precise measurement of the branching ratio and the form factors provide opportunities to test the standard model and the theoretical calculations.

The decay $D^+ \rightarrow \phi e^+\nu_e$ has not been observed at present. The ϕ ($s\bar{s}$) has different quark composition from the D meson ($c\bar{d}$), so the process can only proceed either through $\omega - \phi$ mixing or non-perturbative “weak annihilation” (WA). A measurement of the branching fraction can discriminate which process is dominant.

The signal yields are determined by the variable U , the difference between the missing energy and momentum [8]. The yield of $D^+ \rightarrow \omega e^+\nu_e$ is obtained from a fit to the U distribution as shown in the left plot of Figure 4. And that of $D^+ \rightarrow \phi e^+\nu_e$ is obtained by counting the number in the signal region $[-0.05, 0.07]$ GeV as shown in the right plot, indicating no significant excess of signal events. The results are concluded in Table 1, which are improved compared with previous reports.

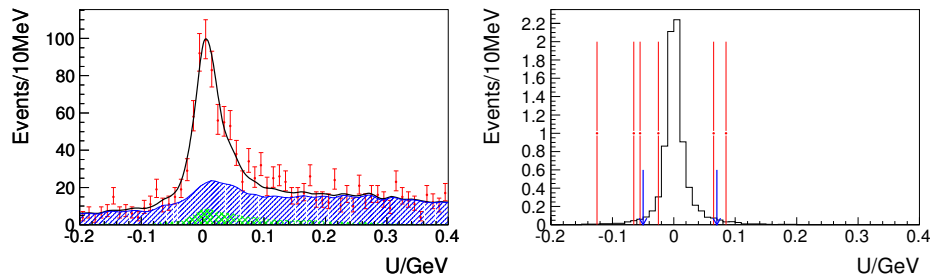


Figure 4: Left: fit (solid line) to the U distribution in data (points with error bars) for $D^+ \rightarrow \omega e^+\nu_e$. The total background is shown by the filled curve, with the peaking component shown by the cross-hatched curve. Right: the U distribution for $D^+ \rightarrow \phi e^+\nu_e$ in data (points with error bars) and signal MC with arbitrary normalization (solid histograms). The arrows show the signal region.

Table 1: Measured branching fractions and a comparison with the previous measurements. For $D^+ \rightarrow \omega e^+\nu_e$, the first uncertainty is statistical and the second systematic.

Mode	This work	Previous [8, 9]
$\omega e^+\nu_e$	$(1.63 \pm 0.11 \pm 0.08) \times 10^{-3}$	$(1.82 \pm 0.18 \pm 0.07) \times 10^{-3}$
$\phi e^+\nu_e$	1.3×10^{-5} (90%C.L.)	9.0×10^{-5} (90%C.L.)

In order to measure the form factors in the decay $D^+ \rightarrow \omega e^+\nu_e$, a five-dimensional maximum likelihood fit is performed in the space of m^2 , q^2 , $\cos\theta_1$, $\cos\theta_2$ and χ , whose definitions are similar with those described for the decay $D^+ \rightarrow K\pi e^+\nu_e$ in

Sec.2. The form factor ratios are determined from the fit: $r_V = 1.24 \pm 0.09 \pm 0.06$, $r_2 = 1.06 \pm 0.15 \pm 0.05$, which are measured for the first time in this decay. The fitted projections over the five variables are illustrated in Figure 5.

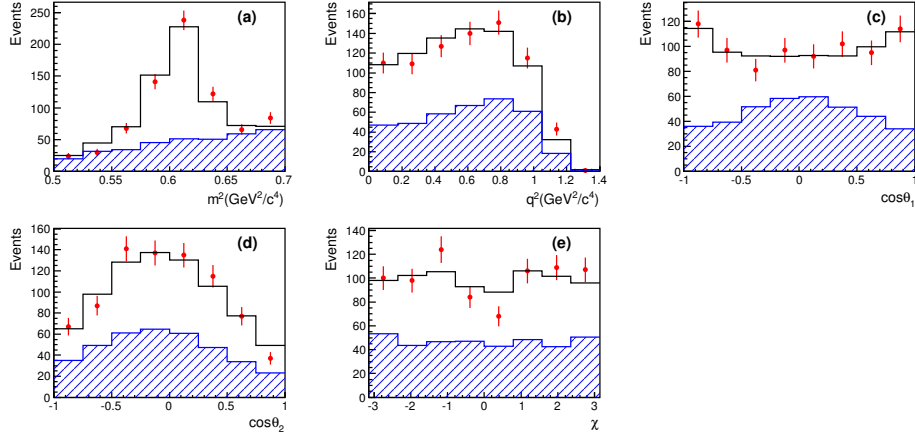


Figure 5: Projections of the data set (points with error bars), the fit results (solid histograms) and the sum of the background distributions (filled histogram curves) onto (a) m^2 , (b) q^2 , (c) $\cos\theta_1$, (d) $\cos\theta_2$ and (e) χ .

4 Study of decay dynamics and CP asymmetry in $D^+ \rightarrow K_L^0 e^+ \nu_e$ decay

In charged D meson decays, CP asymmetry occurs when the absolute value of the decay amplitude for D decaying to a final state is different from the one for the corresponding CP -conjugated amplitude. The most optimistic model-dependent estimates put the SM predictions for the asymmetry as $\mathcal{O}(10^{-3})$ or below [10], so an observation of any CP -violating signal would be a sign of new physics. The hadronic matrix element of D to pseudoscalar meson process can be decomposed into contributions from longitudinal and transverse form factors. Neglecting the lepton mass, only the transverse form factor contributes. Various theoretical techniques provide slightly different q^2 dependencies of the form factors, High precision measurements of the partial decay width over different ranges of q^2 will distinguish which method correctly describes the non-perturbative dynamics of QCD. The $D^+ \rightarrow K_L^0 e^+ \nu_e$ decay is investigated in this work with its branching fraction and CP violation firstly measured. q^2 dependence of the form factors are measured based on different theoretical models for the first time as well.

In the process of searching for $D^+ \rightarrow K_L^0 e^+ \nu_e$ signals, the basic idea for K_L^0 search is explicitly introduced. Most K_L^0 will penetrate the MDC, interact with the scintillators in the EMC and provide the position information. With all charged particles in the event reconstructed and applying energy-momentum conservation to all the particles, the direction of the missing K_L^0 can be determined. We then examine whether there's a good neutral shower deposited in the EMC along the predicted K_L^0 direction.

The signal yield is obtained by fitting the distributions of the beam constrained mass (M_{BC}) of the corresponding tagged D candidates, as illustrated in Figure 6. Branching fractions of the six tag modes are measured separately for D^+ and D^- . Then the weighted branching fractions for D^+ and D^- are obtained: $\mathcal{B}(D^+ \rightarrow K_L^0 e^+ \nu_e) = (4.454 \pm 0.038 \pm 0.102)\%$, $\mathcal{B}(D^- \rightarrow K_L^0 e^- \bar{\nu}_e) = (4.507 \pm 0.038 \pm 0.104)\%$. The combined averaged value is

$$\mathcal{B}(D^+ \rightarrow K_L^0 e^+ \nu_e) = (4.481 \pm 0.027 \pm 0.103)\%, \quad (1)$$

which agrees well with the measurement of $\mathcal{B}(D^+ \rightarrow K_S^0 e^+ \nu_e)$ by CLEO-c [11]. The CP asymmetry is determined to be

$$A_{CP} \equiv \frac{\mathcal{B}(D^+ \rightarrow K_L^0 e^+ \nu_e) - \mathcal{B}(D^- \rightarrow K_L^0 e^- \bar{\nu}_e)}{\mathcal{B}(D^+ \rightarrow K_L^0 e^+ \nu_e) + \mathcal{B}(D^- \rightarrow K_L^0 e^- \bar{\nu}_e)} = (-0.59 \pm 0.60 \pm 1.48)\%, \quad (2)$$

which is consistent with the theoretical prediction in Ref. [12].

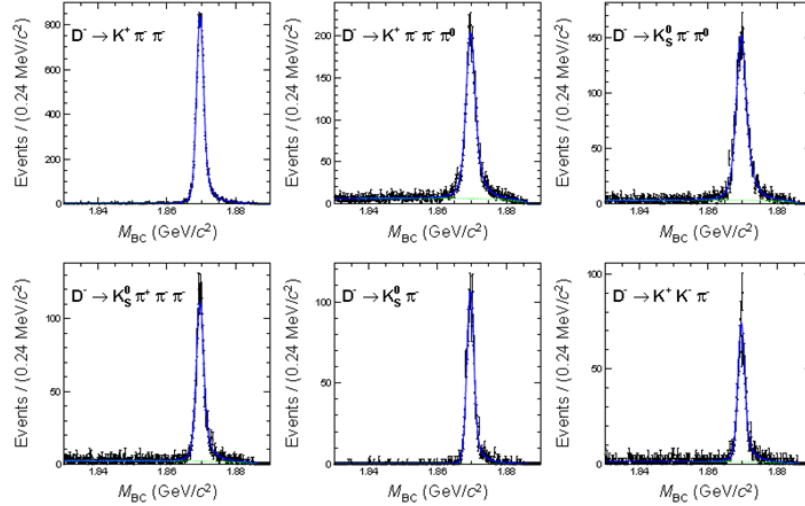


Figure 6: Fits to the M_{BC} distributions of the tagged D^- candidates for data, requiring $D^+ \rightarrow K_L^0 e^+ \nu_e$. The dots with error bars are for data, and the blue solid curves are the results of the fits. The green dashed curves are the fitted backgrounds.

We perform simultaneous fits to the distributions of the observed $D^+ \rightarrow K_L^0 e^+ \nu_e$ candidates as a function of q^2 to determine the product of the hadronic form factor and the CKM matrix element $f_+^K(0)|V_{cs}|$. The form-factor shape is described based on the simple pole model (m_{pole}), the modified pole model (α), two-parameter series expansion (r_1), and three-parameter series expansion (r_1, r_2). As an example, Figure 7 shows the simultaneous fits using the two-parameter series expansion model, corresponding to the results: $f_+^K(0)|V_{cs}| = 0.728 \pm 0.006 \pm 0.011$, $r_1 = -1.91 \pm 0.33 \pm 0.24$.

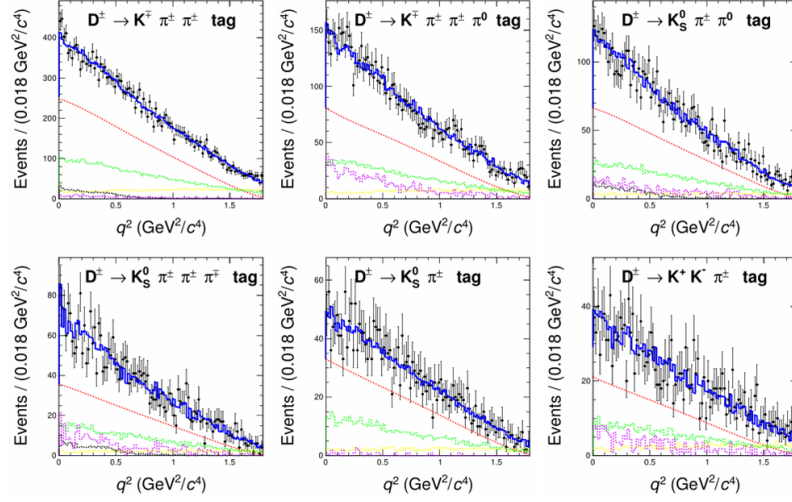


Figure 7: (Color online) Simultaneous fits (blue solid curves) to the numbers of $D^+ \rightarrow K_L^0 e^+ \nu_e$ data (points with error bars) as a function of q^2 with the two-parameter series expansion parameterization. The red dashed curves show the signal, while the violet, yellow, green and black curves refer to different kinds of backgrounds.

5 Summary

Based on 2.92 fb^{-1} of data collected by the BESIII experiment three semileptonic decays are analysed. In the study of $D^+ \rightarrow K^- \pi^+ e^+ \nu_e$, its branching fractions are measured: $\mathcal{B}(D^+ \rightarrow K^- \pi^+ e^+ \nu_e) = (3.71 \pm 0.03 \pm 0.08)\%$, $\mathcal{B}(D^+ \rightarrow K^- \pi^+ e^+ \nu_e)_{[0.8,1]} = (3.33 \pm 0.03 \pm 0.07)\%$. A PWA is performed and an S -wave contribution is found to account for $(6.05 \pm 0.22 \pm 0.18)\%$. The S -wave phase and the form factors are measured both by the PWA and in a model-independent way, showing good consistency. For the decay $D^+ \rightarrow \omega e^+ \nu_e$, the branching fraction is measured with a higher precision: $\mathcal{B}(D^+ \rightarrow \omega e^+ \nu_e) = (1.63 \pm 0.11 \pm 0.08)\%$. Its form factors are determined for the first time: $r_V = 1.24 \pm 0.09 \pm 0.06$, $r_2 = 1.06 \pm 0.15 \pm 0.05$. The rare decay $D^+ \rightarrow \phi e^+ \nu_e$ is

searched for and an upper limit at 90% confidence level is set: $\mathcal{B}(D^+ \rightarrow \phi e^+ \nu_e) < 1.3 \times 10^{-5}$. For the decay $D^+ \rightarrow K_L e^+ \nu_e$, we present the first measurement of the absolute branching fraction $\mathcal{B}(D^+ \rightarrow K_L^0 e^+ \nu_e) = (4.481 \pm 0.027 \pm 0.103)\%$. The CP asymmetry is also determined $A_{CP} = (-0.59 \pm 0.60 \pm 1.48)\%$, indicating no significant CP violation. The product $f_+^K(0)|V_{cs}|$ is measured based on three theoretical form-factor models. Taking the two-parameter series expansion parameterization, $f_+^K(0)|V_{cs}| = 0.748 \pm 0.007 \pm 0.012$.

ACKNOWLEDGEMENTS

This work is supported in part by National Natural Science Foundation of China (NSFC) under Contracts Nos. 11075174, 11475185.

References

- [1] M. Ablikim *et al.* (BESIII Collaboration), Chin. Phys. C **37**, 123001 (2013).
- [2] M. Ablikim *et al.*, Nucl. Instrum. Meth. A **614**, 345 (2010).
- [3] R.M. Baltrusaitis *et al.*, Phys. Rev. Lett. **56**, 2140 (1986).
- [4] C. W. Bernard, A. X. El-Khadra and A. Soni, Phys. Rev. D **45**, 869 (1992);
- [5] N. Cabibbo and A. Maksymowicz, Phys. Rev. B **137**, 438 (1965).
- [6] J.M. Link *et al.* (FOCUS Collaboration), Phys. Lett. B **633**, 183 (2006).
- [7] R.A. Briere *et al.* (CLEO Collaboration), Phys. Rev. D **81**, 112001 (2010).
- [8] S. Dobbs *et al.* (CLEO Collaboration), Phys. Rev. Lett. **110**, no. 13, 131802 (2013).
- [9] J. Yelton *et al.* (CLEO Collaboration), Phys. Rev. D **84**, 032001 (2011).
- [10] F. Buccella, M. Lusignoli, G. Miele, A. Pugliese and P. Santorelli, Phys. Rev. D **51**, 3478 (1995); Y. Grossman, A. L. Kagan and Y. Nir, Phys. Rev. D **75**, 036008 (2007).
- [11] D. Besson *et al.* [CLEO Collaboration], Phys. Rev. D **80**, 032005 (2009).
- [12] Z. Z. Xing, Phys. Lett. B **353**, 313 (1995); Phys. Lett. B **363**, 266 (1995).